Proceedings of the
8th Graz Brain-Computer Interface Conference 2019 DOI: 10.3217/978-3-85125-682-6-11

# ASYNCHRONOUS DETECTION OF ERROR-RELATED POTENTIALS USING A GENERIC CLASSIFIER

C Lopes-Dias[1], A I Sburlea[1], G R Müller-Putz[1]

[1]Institute of Neural Engineering, Graz University of Technology, Graz, Austria

E-mail: gernot.mueller@tugraz.at

ABSTRACT: Error-related potentials (ErrPs) can be used to improve BCIs' performance but its use is often withheld by long calibration periods. We recorded EEG data of 15 participants while controlling a robotic arm towards a target. In 30 % of the trials, the protocol prompted an error during the trial in order to trigger ErrPs in the participants. For each participant, we trained an ErrP classifier using the data of the remaining 14 participants. Each of these classifiers was tested asynchronously on the data of the selected participant. The threshold that maximized the product of the average true positive rate (TPR) and the average true negative rate (TNR) was $\tau = 0.7$. For this threshold, the average TPR was 53.6 % and the average TNR was 82.0 %. These results hint at the feasibility of transferring ErrPs between participants as a reliable strategy to reduce or even remove the calibration period when training ErrP classifiers to be used in an asynchronous manner.

## INTRODUCTION

Brain-computer interfaces (BCIs) are a suitable tool to help restoring some autonomy to people with severe motor disabilities [1,2,3]. Most BCIs rely on converting modulated brain activity of a user (often measured using electroencephalography (EEG)) into commands of an external device, such as a robot. Nevertheless, the performance of most BCIs is not optimal and, occasionally, the interface misinterprets the intention of its user and thus a wrong command is executed. The user's awareness of the committed mistake is associated with a neural pattern named error-related (ErrP), which is also measurable by EEG [4] .

Incorporating ErrPs' detection in a BCI can help to improve its performance [5, 6]. A main barrier to its widespread use is the calibration time necessary to train ErrP classifiers: many trials are needed to train a classifier and errors should not occur too often to still be perceived as so. Two main approaches have been proposed to reduce the training duration of ErrP classifiers, based on either transferring information between different tasks or transferring information between different participants. Iturrate and colleagues studied the use of classifiers trained with ErrPs from one observation task and tested in ErrPs from another observation task, using latency correction [7,8]. Kim and colleagues studied the use of an ErrP classifier trained with ErrPs from an observation task and tested with ErrPs from an interaction task (and vice-versa) [9,10]. Nevertheless, Ehrlich and colleagues, did not recommend re-using ErrP classifiers across different experimental tasks [11]. Kim and colleagues also studied the use of an ErrP classifier trained with ErrPs from several subjects and tested in ErrPs from another subject [9]. These studies suggest that transferability of ErrPs is viable in the context of discrete BCIs (in which all events occur in a discrete way).

Recently, an effort has been made to develop BCI paradigms that promote a smoother and more intuitive interaction with their users, by relying on continuous control or actions - continuous BCIs [12,13,14]. In this context, the user's error awareness can occur at any moment and is not, necessarily, time-locked to specific events, requiring an asynchronous detection of ErrPs. The existence of ErrPs in continuous contexts as well as its asynchronous detection has been established [15, 16, 17,18].

Another approach to improve BCIs consists in developing BCIs that closer resemble end-user applications, in which users interact with or observe robots [10,19,20,21,22].

In this work, we developed a paradigm in which the user has continuous control over a robotic arm in a task in which errors are triggered by the paradigm. We studied the electrophysiological signature of the ErrPs in this task and, additionally, investigated the feasibility of using a generic ErrP classifier trained on the ErrPs of 14 participants by testing it asynchronously with data of another participant.

## MATERIALS AND METHODS

*EEG recording:* We recorded EEG and EOG data at a sampling frequency of 500 Hz, using BrainAmp amplifiers (Brain Products, Munich, Germany). We used 61 EEG electrodes and 3 EOG electrodes. The EEG electrodes were placed at positions Fp1, Fp2, AF3, AF4, F7, F5, F3, F1, Fz, F2, F4, F6, F8, FT7, FC5, FC3, FC1, FCz, FC2, FC4, FC6, FT8, T7, C5, C3, C1, Cz, C2, C4, C6, T8, TP9, TP7, CP5, CP3, CP1, CPz, CP2, CP4, CP6, TP8, TP10, P7, P5, P3, P1, Pz, P2, P4, P6, P8, PO9, PO7, PO3, POz, PO4, PO8, PO10, O1, Oz, and O2. The ground electrode was placed at position AFz and the reference electrode was placed on the right mastoid. The electrodes were placed above the nasion and below the

 DOI: 10.3217/978-3-85125-682-6-11

outer canthi of the eyes.

*Participants:* We recorded 15 right-handed healthy volunteers (5 female). The participants were, on average, 23.4 ± 2.5 years old (mean ± std). Participants were paid 7.50 € per hour and, before the experiment, read and signed an informed consent form that was previously accepted by the local ethical committee.

*Experiment layout:* Figure 1 depicts the layout of the experiment. Participants sat in front of a table, with their right hand lying flat on the table, covered by a wooden structure. On the ceiling of this structure was a Leap Motion device that tracked their right hand movements (Leap Motion, San Francisco, USA). On the right of the participants was a robotic arm (Jaco Assistive robotic arm - Kinova Robotics, Bonn, Germany). On top of the wooden structure were two violet boxes representing the physical targets, centred in relation to the home position of the robot's hand. Behind the wooden structure was a monitor that displayed information regarding the experiment. During the trials, the participants could control the position of the robot's hand on an approximately horizontal plan, by moving their right hand on the table. We considered robot's hand displacement to be three times bigger than the participants' hand displacement, to reduce the range of the participants' movements.

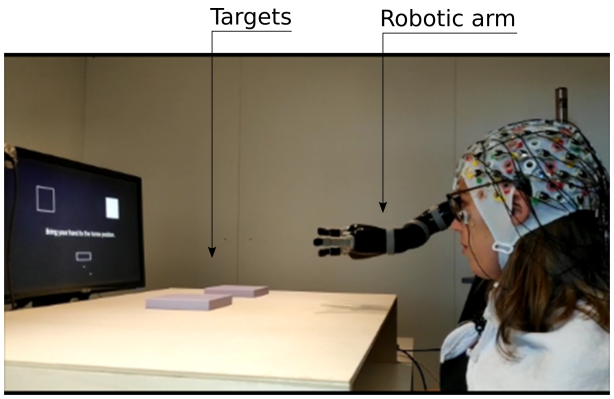


Figure 1: Experimental setup during the pre-trial period. In this image, the robot is at its home position. The squares on the screen indicate that, in the next trial, the participant should move the robot's hand towards the right target (purple box) on the wooden structure. The screen also shows the home position for the participant's hand (rectangle on the bottom part of the screen). The text on the screen (not readable in the picture) states 'Bring your hand to the home position'.

*Experiment overview:* The experiment consisted of 8 blocks of 30 *trials* each. Each block contained 21 *correct trials* and 9 *error trials* (70% and 30%, respectively). The position of the error trials within the block was randomly generated, using an uniform distribution.

*Pre-trial period:* During this period, on the upper part of the screen were displayed two squares, representing the two targets on the wooden structure. One of the squares was filled in white, representing the selected target for the next trial, and the other had no fill. On the bottom part of the screen was a rectangle representing

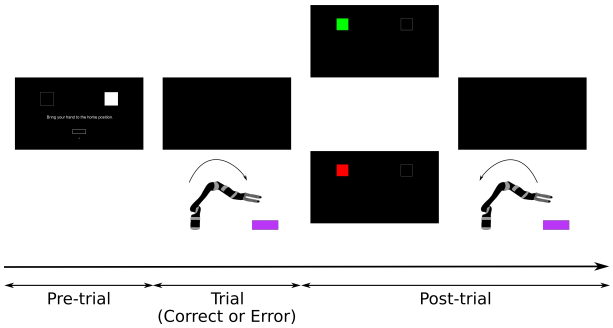


Figure 2: Experimental protocol. During the pre-trial period, the participants can rest for as long as they wish. The pre-trial period ends and a trial starts, when the participant brings his/her right hand to its home position (the bottom rectangle). During the trials, the screen is black. The participants were instructed to bring the robot's hand to the selected target (indicated by the white square). A trial finishes either when the robot reaches the target or after 6 seconds (if the target was not reached). Afterwards (post-trial), the squares reappear on the screen for 1.5 seconds and give feedback regarding hitting the target (a green square indicates that the target was hit and a red square indicates that the target was not hit). Then the screen turns black and the robot automatically returns to its home position and a new pre-trial period starts.

the home position for the participants' hand. The participants' hand was represented by a dot on the screen. A new trial started when the participants' hand entered its home position. The participants could use the pre-trial period to rest for as long as they needed. Participants were instructed to bring their hand to below the home position, to fixate their gaze on the selected physical target and to enter the home position when they felt ready to start a new trial. Participants were also instructed not to move their gaze during the entire trial duration, in order to minimize eye movements.

*Trials:* The aim of each trial was to move the robot's hand to the selected target. During the trials, the screen was black. A trial finished when the robot's hand was above the target (hit) or after 6 seconds (no hit). Afterwards, as shown in Figure 2, the two squares from the pre-trial period reappeared on the screen for 1.5 seconds and the previously filled square was now filled in either green (hit) or red (no hit). Then, the screen would turn black, the robot's hand would automatically move to its home position and a new pre-trial period would start.

*Error trials:* In these trials, the paradigm triggered an *error* during the trial. The *error* consisted on halting the participant's control of the robot and adding a 5 cm upwards displacement to the robot's hand.The errors occurred randomly when the robot's hand was within 25 % to 65 % of the minimal forward displacement necessary for the robot to hit the target. Participants perceived the error by noticing the robot stopping and lifting. After the error happened, the participants could not control the robot until the trial ended. Participants were instructed to remain still. The error trials lasted 6 seconds.

*Correct trials:* In these trials, no error was triggered by the paradigm. The participants reached the selected target

 DOI: 10.3217/978-3-85125-682-6-11

in $99.7 \pm 0.5$ % (mean $\pm$ std) of the correct trials. Correct trials lasted, on average, $2.06 \pm 0.17$ seconds (mean $\pm$ std).

*Preprocessing the data:* The eye movements and blinks were removed from the EEG data, using the artefact subspace subtraction algorithm [23]. The EEG data was then filtered between 1 and 10 Hz with a Butterworth causal filter of order 4.

*Electrophysiological analysis:* For the electrophysiological analysis, we cut the EEG data in 1.5 s epochs. For the error trials, we considered the interval [-0.5, 1]s time-locked to the error onset (0 s). Since correct trials have no intrinsic onset, we defined a virtual onset, occurring one second after the start of the trial (at a time-point in which errors could already occur). For the correct trials we considered the interval $[-0.5, 1]$s, time-locked to the virtual onset (0 s).

*Asynchronous ErrP classification with a generic classifier:* For every participant we trained an ErrP classifier with two classes (correct and error) using the data from the remaining 14 participants. In order to train each of these classifiers, we considered as features for the error class the amplitudes of all EEG channels at all time points within the window $[0.30, 0.75]$s after the error onset. Similarly, we considered as features for the correct class the amplitudes of all EEG channels at all time points within the window $[0.30, 0.75]$s after the virtual onset. Afterwards, in order to reduce the number of features, we applied principal component analysis (PCA) to the feature matrix and kept the components that preserved 99 % of the data variance. These components were used to train a shrinkage LDA classifier [24]. Each of these classifiers was tested asynchronously in the data of the participant not used for training. For that, we slid a 450 ms window through the trials, obtaining an output from the classifier every 18 ms.

For every fixed threshold $\tau$ ($\tau$ from 0 to 1 in steps of 0.025), we considered an *error detection* when the classifier's probability for the error class ($p_e$) was greater or equal to the threshold $\tau$ for two consecutive windows ($p_e \geq \tau$). As an evaluation metric for the asynchronous classification, we defined as true negative trials (TN trials) the correct trials in which no error detection occurred. We defined as true positive trials (TP trials), the error trials in which no error detection occurred before the error onset and at least one error detection occurred within 1.5 seconds after the error onset. We considered the group performance to be optimal for the threshold that maximized the product of the average TPR and the average TNR.

## RESULTS

Figure 3 displays the grand average correct and error signals at channel FCz (green and red solid lines respectively). The 95 % confidence interval for the average curves are represented by the shaded green and red areas. The time-regions in which correct and error signals were significantly different are represented by grey shaded areas (Wilcoxon signed-rank tests, $p < 0.01$, Bonferroni corrected). Figure 3 displays also the topoplots for the correct and error grand average signals at the peaks of the grand average error signal ($t$ =0.354 s and $t = 0.568$ s).

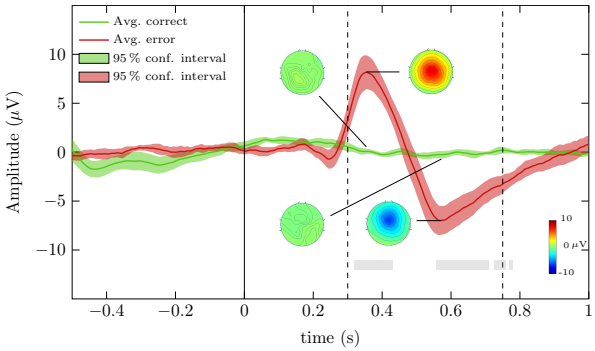


Figure 3: Grand average correct and error signal at channel FCz (green and red solid lines, respectively). The shaded areas represent the 95 % confidence interval for the average signals. The grey regions represent the time-regions in which correct and error signals were significantly different (Wilcoxon signed-rank tests, $p < 0.01$, Bonferroni corrected).The topoplots for the correct and error grand average signals are displayed for $t$ =0.354 s and $t = 0.568$ s. The time point $t = 0$ represents the error onset of error trials and the virtual onset of correct trials

Figure 4 shows the average true negative rate (TNR) and the average true positive rate (TPR) (represented with green and red solid lines, respectively), for all the tested thresholds in the asynchronous ErrP classification with a generic classifier. The chance-level TNR and TPR were calculated by performing the same classification procedure with shuffled training labels. The 95 % confidence intervals for the average curves are represented by shaded areas. The threshold that maximized the group performance was $\tau = 0.700$. For this threshold, the average TNR was 82.0 % and the average TPR was 53.6 %.
Figure 5 depicts the individual TNR and TPR of each participant. It depicts also the threshold that maximizes group performance ($\tau = 0.700$, grey dashed lines) and the thresholds that maximizes the individual performance (blue dashed lines).

## DISCUSSION

We developed an experimental task relying on continuous control of a robot towards a target. In 30 % of the trials (error trials), an error was triggered by the paradigm, causing the participants to loose control over the robot during the trial. We then studied the electrophysiological features associated with the error trials. The peaks of the error signal occurred at $t$ =0.354 s and $t$ =0.568 s. Our results are not directly comparable with state-of-the-art literature because we processed the EEG signal with a causal filter, causing the N200 component of the ErrP to shift to around 600 ms. We decided to keep the causal filter because it depicts the ErrP's shape in the scenario of an online ErrP decoder, bringing awareness to the fact that ERP shapes can be influenced by the filter used to

 DOI: 10.3217/978-3-85125-682-6-11

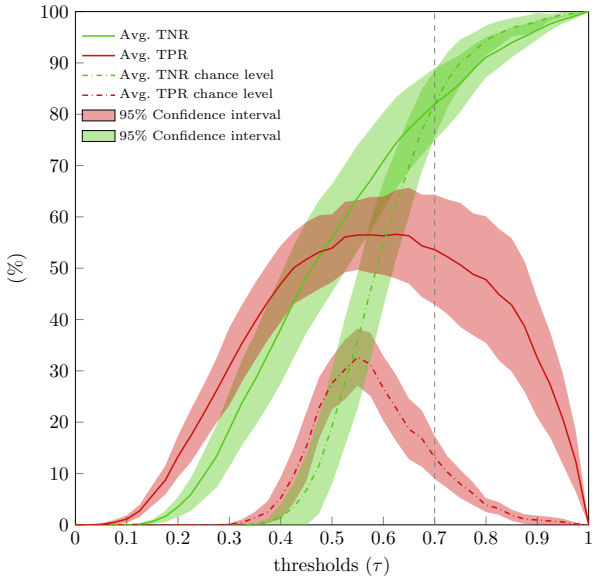


Figure 4: Average TNR and average TPR (green and red solid lines, respectively) for the different thresholds tested in the asynchronous ErrP classification with a generic classifier. The chance-level TNR and TPR are depicted with green and red dashed lines. The shadowed areas represent the 95 % confidence intervals for the average curves. The threshold that maximizes the group performance is represented with a grey vertical dashed line.

process the signal.

Afterwards, we evaluated the feasibility of transferring ErrP information across participants, by training a classifier with the data from 14 participants and testing it with the data of the remaining participant in an asynchronous manner (generic classifier). From Figure 4, we observe that the average TPR is above chance-level for all the thresholds and that the average TNR is increasing with the threshold. This points to the feasibility of using such classifiers as a starting point for an adaptive BCI. In Figure 5, it is possible to compare the individual performance of every participant with the generic classifier. We observe that participants with higher individual threshold present minor or negligible drops in performance with the use of a generic classifier tuned to the group performance (e.g. participants 1, 2 and 3). On the other hand, participants with lower individual threshold can present major performance drops (e.g. participants 5 and 8). This indicates that the performance of such classifier is still determined by individual characteristics of the participants. Nevertheless it seemed a suitable option for the majority of the participants.

## CONCLUSION

In this work we showed the feasibility of transferring ErrP information across participants, by training a classifier with the data from 14 participants and testing it with the data of the remaining participant in an asynchronous manner. We then showed that, although the performance of such classifiers is still dependent on individual characteristics of the participants, the majority of them would benefit from such generic approach. Therefore, we believe that transferring ErrP information across participants is a viable alternative to reduce the calibration period in a scenario of asynchronous ErrP classification, as a starting point for an adaptive BCI.

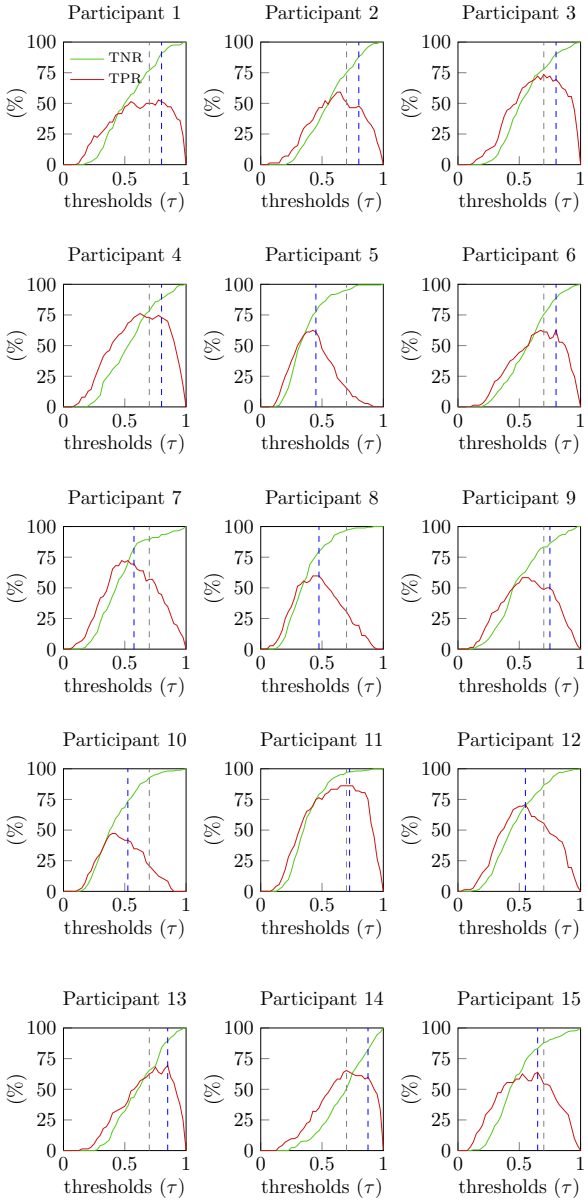


Figure 5: Individual TNR and TPR (green and red solid lines, respectively) for the different thresholds tested in the asynchronous ErrP classification with a generic classifier. The threshold that maximizes the group performance is represented with a grey dashed line ($\tau = 0.7$). The threshold that maximizes the individual performance is represented with a blue dashed line.

## ACKNOWLEDGEMENTS

The authors would like to acknowledge the fruitful discussions with the members of 'Feel Your Reach'. This work was supported by Horizon 2020 ERC Consolidator

 DOI: 10.3217/978-3-85125-682-6-11

Grant 681231 'Feel Your Reach'.

REFERENCES

[1] Millán JdR et al. Combining Brain–Computer Interfaces and Assistive Technologies: State-of-the-Art and Challenges. Frontiers in Neuroscience 2010; 4:161.
[2] Müller-Putz G et al. Towards Noninvasive Hybrid Brain–Computer Interfaces: Framework, Practice, Clinical Application, and Beyond, in Proc. of the IEEE, 2015, 103(6), 926-943.
[3] Müller-Putz GR et al. Towards non-invasive brain-computer interface for hand/arm control in users with spinal cord injury, in Proc. 5th International Winter Conference on Brain-Computer Interface (BCI), Sabuk, 2017, 63-65.
[4] Chavarriaga R, Sobolewski A, Millán JdR. Errare machinale est: the use of error-related potentials in brain-machine interfaces. Frontiers in Neuroscience 2014; 8:208.
[5] Schmidt NM, Blankertz B, Treder MS. Online detection of error-related potentials boosts the performance of mental typewriters. BMC Neuroscience. 2012; 13(1):13-19.
[6] Spüler M, Bensch M, Kleih S, Rosenstiel W, Bogdan M, Kübler A. Online use of error-related potentials in healthy users and people with severe motor impairment increases performance of a P300-BCI. Clinical Neurophysiology. 2012; 123(7):1388-1337.
[7] Iturrate, I, Chavarriaga R, Montesano L, Minguez J, Millán JdR. Latency correction of error-related potentials reduces BCI calibration time, in Proc. of the 6th International Brain-Computer Interface Conference, Graz, Austria, 2014.
[8] Iturrate I, Chavarriaga R, Montesano L, Minguez J, Millán JdR. Latency correction of event-related potentials between different experimental protocols. Journal of Neural Engineering 2014; 11(3):036005.
[9] Kim SK, Kirchner EA. Handling few training data: classifier transfer between different types of error-related potentials. IEEE Transactions on Neural Systems and Rehabilitation Engineering. 2016, 24(3):320-332.
[10] Kim SK, Kirchner EA, Stefes A, Kirchner F. Intrinsic interactive reinforcement learning – Using error-related potentials for real world human-robot interaction. Scientific Reports. 2017, 7:17562.
[11] Ehrlich S, Cheng G. A Feasibility Study for Validating Robot Actions Using EEG-Based Error-Related Potentials International Journal of Social Robotics. 2018.
[12] Doud AJ, Lucas JP, Pisansky MT, He B. Continuous three-dimensional control of a virtual helicopter using a motor imagery based brain-computer interface. PLOS ONE. 2011; 6(10):e26322.
[13] Coyle D, Garcia J, Satti A, Mcginnity TM. EEG-based continuous control of a game using a 3 channel motor imagery BCI: BCI game. in 2011 IEEE Symposium on Computational Intelligence, Cognitive Algorithms, Mind, and Brain (CCMB), Paris, France, 2011, 1-7.
[14] Galán F et al. A brain-actuated wheelchair: Asynchronous and non-invasive Brain–computer interfaces for continuous control of robots. Clinical Neurophysiology. 2008; 119(9):2159 - 2169.
[15] Omedes J, Iturrate I, Minguez J, Montesano L. Analysis and asynchronous detection of gradually unfolding errors during monitoring tasks. Journal of Neural Engineering 2015; 12(5):056001.
[16] Omedes J, Iturrate I, Chavarriaga R, Montesano L. Asynchronous Decoding of Error Potentials during the Monitoring of a Reaching Task 2015 IEEE International Conference on Systems, Man, and Cybernetics, Kowloon, 2015, 3116-3121.
[17] Spüler M, Niethammer C. Error-related potentials during continuous feedback: using EEG to detect errors of different type and severity. Frontiers in Human Neuroscience. 2015; 9:155.
[18] Lopes-Dias C, Sburlea AI, Müller-Putz GR. Masked and unmasked error-related potentials during continuous control and feedback. Journal of Neural Engineering. 2018; 15(3):036031.
[19] Kreilinger A, Neuper C, Müller-Putz G. Error potential detection during continuous movement of an artificial arm controlled by brain-computer interface.Med Biol Eng Comput. 2012; 60:223.
[20] Iturrate I, Chavarriaga R, Montesano L, Minguez J, Millán JdR. Latency correction of error potentials between different experiments reduces calibration time for single-trial classification, in 2012 Annual International Conference of the IEEE Engineering in Medicine and Biology Society, San Diego, CA, 2012, 3288-3291.
[21] Salazar-Gomez AF, DelPreto J, Gil S, Guenther FH, Rus D. Correcting robot mistakes in real time using EEG signals, in 2017 IEEE International Conference on Robotics and Automation (ICRA), Singapore, 2017, 6570-6577.
[22] Ehrlich SK, and Cheng G. Human-agent co-adaptation using error-related potentials. Journal of Neural Engineering. 2018; 15(6):066014.
[23] Kobler RJ, Sburlea AI, Müller-Putz GR. A comparison of ocular artifact removal methods for block design based electroencephalography experiments, in Proc. of the 7th International Brain-Computer Interface Conference, Graz, 2017, 236-241.
[24] Blankertz B, Lemm S, Trede M, Haufe S, and Müller KR. Single-trial analysis and classification of ERP components — A tutorial. NeuroImage; 2011 56(2):814 - 825.